Affective Science (2022) 3:406–424
https://doi.org/10.1007/s42761-021-00098-y

RESEARCH ARTICLE

Multivariate Brain Activity while Viewing and Reappraising Affective Scenes Does Not Predict the Multiyear Progression of Preclinical Atherosclerosis in Otherwise Healthy Midlife Adults

Peter J. Gianaros[1] · Javier Rasero[2] · Caitlin M. DuPont[1] · Thomas E. Kraynak[1] · James J. Gross[3] · Kateri McRae[4] · Aidan G.C. Wright[1] · Timothy D. Verstynen[2] · Emma Barinas-Mitchell[5]

Received: 13 July 2021 / Accepted: 17 December 2021 / Published online: 19 February 2022

Abstract

Cognitive reappraisal is an emotion regulation strategy that is postulated to reduce risk for atherosclerotic cardiovascular disease (CVD), particularly the risk due to negative affect. At present, however, the brain systems and vascular pathways that may link reappraisal to CVD risk remain unclear. This study thus tested whether brain activity evoked by using reappraisal to reduce negative affect would predict the multiyear progression of a vascular marker of preclinical atherosclerosis and CVD risk: carotid artery intima-media thickness (CA-IMT). Participants were 176 otherwise healthy adults (50.6% women; aged 30–51 years) who completed a functional magnetic resonance imaging task involving the reappraisal of unpleasant scenes from the International Affective Picture System. Ultrasonography was used to compute CA-IMT at baseline and a median of 2.78 (interquartile range, 2.67 to 2.98) years later among 146 participants. As expected, reappraisal engaged brain systems implicated in emotion regulation. Reappraisal also reduced self-reported negative affect. On average, CA-IMT progressed over the follow-up period. However, multivariate and cross-validated machine-learning models demonstrated that brain activity during reappraisal failed to predict CA-IMT progression. Contrary to hypotheses, brain activity during cognitive reappraisal to reduce negative affect does not appear to forecast the progression of a vascular marker of CVD risk.

Keywords Cardiovascular disease risk · Cognitive reappraisal · Emotion regulation · fMRI · Machine learning · Negative affect

Negative affect may confer risk for atherosclerotic cardiovascular disease (CVD; Kraynak et al., 2018; Suls, 2018). Acute experiences of negative affect, for example, increase the likelihood of ischemic events, arrhythmias, and sudden cardiac death among vulnerable individuals (Jiang, 2015; Kamarck & Jennings, 1991; Lampert, 2016; Steptoe & Brydon, 2009). In addition to acute affective states, an individual's propensity to experience negative affect also appears to confer risk for CVD endpoints (e.g., early death; Kubzansky et al., 2005; Rozanski et al., 1999) and for an accelerated progression of preclinical atherosclerosis (Stewart et al., 2007). The CVD risk conferred by negative affect may be due—at least in part—to its maladaptive or insufficient regulation (DeSteno et al., 2013; Kubzansky et al., 2011); however, the deliberate regulation of negative affect *per se* is rarely examined in the context of CVD risk.

One affective regulation strategy that is postulated to reduce CVD risk is cognitive reappraisal (Appleton & Kubzansky, 2014; Gianaros & Jennings, 2018). Cognitive reappraisal involves intentionally changing the meaning of events and contexts with the goal of changing affective responses (Gross, 2014). Four lines of evidence suggest that individual differences in reappraisal processes may relate to biological and behavioral risk factors for CVD. First, in clinical contexts, reappraisal training is a component of adjunctive

Handling Editor: Kristen Lindquist

✉ Peter J. Gianaros
gianaros@pitt.edu

[1] Department of Psychology, University of Pittsburgh, Pittsburgh, PA, USA

[2] Department of Psychology, Carnegie Mellon University, 3131 Sennott Square, 210 S. Bouquet St, Pittsburgh, PA, USA

[3] Department of Psychology, Stanford University, Stanford, CA, USA

[4] Department of Psychology, University of Denver, Denver, CO, USA

[5] Department of Epidemiology, University of Pittsburgh, Pittsburgh, PA, USA

cognitive-behavioral programs designed to reduce CVD risk in patient populations (Cohen et al., 2015). Second, in epidemiological studies, the self-reported frequency of using reappraisal in daily life has been positively associated with cardioprotective health behaviors and negatively associated with lipid and inflammatory biomarkers of CVD risk (Appleton et al., 2013; Appleton et al., 2014; Ellis et al., 2019). Third, across psychophysiological studies, meta-analytic evidence suggests that reappraisal decreases acute cardiovascular—namely, heart rate—reactions to unpleasant stimuli (Zaehringer et al., 2020). Heart rate reactions to unpleasant, stressful, or otherwise aversive stimuli and contexts have been associated separately with the severity of atherosclerosis in nonhuman primates (Manuck et al., 1983) and biological markers of atherosclerosis and CVD risk in humans (Chida & Steptoe, 2010; Gianaros & Jennings, 2018; Turner et al., 2020). Fourth, neuroimaging findings from a sample of 157 midlife adults indicate that activity in the medial prefrontal cortex, particularly in the dorsal anterior cingulate cortex (dACC), during reappraisal cross-sectionally associates with systemic inflammation and preclinical atherosclerosis (Gianaros et al., 2014). In aggregate, clinical efforts and findings from epidemiological, psychophysiological, and neuroimaging studies appear compatible with speculations that reappraisal may relate to CVD risk via neural, behavioral, and physiological pathways that influence the heart and vasculature.

In the latter regards, it is notable that reappraisal not only engages the dACC (Buhle et al., 2014) and other prefrontal areas (Wager et al., 2008), but also a distributed ensemble of brain systems whose activity relates to (i) processing affective stimuli (Lindquist et al., 2012) and (ii) controlling and representing autonomic, neuroendocrine, cardiovascular, and immune parameters of physiology that are involved in the early etiology of CVD (Kraynak et al., 2018). The latter processes are thought to be instantiated in an ensemble of brain systems for visceral control that calibrate peripheral physiology with the anticipated (predicted) metabolic demands of self-relevant contexts (Koban et al., 2021; Quigley et al., 2021). This ensemble includes areas of the insula, orbital and medial prefrontal cortex, amygdala, hippocampus, and cell groups of the brainstem that could plausibly link affective processes with physical health, particularly cardiovascular health (Koban et al., 2021; Öngür & Price, 2000). As evidence, for example, distributed (multivariate) activity patterns across this ensemble and other brain systems that are evoked by negative affective stimuli (unpleasant visual scenes) associate with baseline (cross-sectional) levels of a vascular marker of preclinical atherosclerosis, namely, carotid artery intima-media thickness CA-IMT; (Gianaros et al., 2020).

Baseline levels of CA-IMT are associated with the incident (future) development of atherosclerotic plaques, and they are interpreted to reflect the effects of CVD risk factors that have accrued over the lifespan (Tschiderer et al., 2020). By comparison to such cumulative effects, the *rate-of-change* in CA-IMT over time (e.g., years) is thought to reflect the more recently experienced influence of proximal etiological determinants of the progression of preclinical atherosclerosis (Chambless et al., 2002). Various metrics reflecting the rate-of-change in CA-IMT appear to be modifiable by behavioral and pharmacological interventions, and they predict clinical CVD endpoints in epidemiological studies (Baldassarre et al., 2013; Willeit et al., 2020). An open question about the neurobiology of the pathways potentially linking affect and affect regulation to CVD risk is whether distributed brain activity patterns that are evoked by negative affective stimuli and by reappraisal predict the prospective rate-of-change in CA-IMT over multiple years. If so, then such findings would extend prior cross-sectional findings by providing initial evidence as to whether the neural correlates of negative affect and its regulation by reappraisal at a given point in time are able to forecast (predict) the future progression of a precursor to later clinical CVD endpoints: preclinical atherosclerosis.

Accordingly, the present study assessed brain activity by functional magnetic resonance imaging (fMRI) among a community sample of 176 otherwise healthy adults (89 women, 87 men; aged 30 to 51 years), while they viewed and reappraised unpleasant scenes from the International Affective Picture System. At the time of initial testing and then a median of 2.78 (interquartile range, 2.67 to 2.98) years later, ultrasonography was used to assess CA-IMT among those who returned for follow-up testing (N = 146; 78 women, 68 men; 83% retention). At the time of initial testing, participants were not taking medications and were not diagnosed with clinical (e.g., cardiovascular) conditions that might confound initial (baseline) CA-IMT levels. Whole-brain, multivariate, and penalized regression analyses with dimensionality reduction and cross-validation (Kohoutova et al., 2020) were used to test whether fMRI patterns evoked by viewing and reappraising unpleasant scenes at the time of initial testing predicted the change in CA-IMT over the multiyear follow-up interval. Ancillary analyses explored the psychometric properties of fMRI patterns and affective responses evoked by viewing and reappraising the visual scenes, as well as the potential influence of conventional CVD risk factors and self-reports of negative affect on any associations observed between fMRI patterns and CA-IMT.

Method

Preregistration and Availability of Code and Data

Hypotheses and planned analyses were preregistered at Open Science Framework (OSF) on 02 November 2020 (https://osf.io/hk6qx/). Subsequently created data files and

analysis scripts are available at OSF (https://osf.io/hk6qx/) and GitHub (https://github.com/CoAxLab/reappraisal-imt-progression). Group and individual neuroimaging data and results are available at NeuroVault (https://neurovault.org/collections/10337). To the authors' awareness, this is the first study to report associations between affect-related brain patterns and longitudinal changes in CA-IMT.

Participants

Participants were midlife and community-dwelling adults from the Pittsburgh Imaging Project (PIP), a longitudinal study of biological and behavioral risk factors for preclinical atherosclerosis and CVD risk. The entire PIP cohort consists of 331 individuals (aged 30 to 51 years; 166 women and 165 men; 230 identifying as white; 80 identifying as Black or African American; 16 identifying as Asian or Asian American; and 5 identifying as multiracial). Details regarding recruitment, study design, and dates of data collection have been published (Gianaros et al., 2017; Gianaros et al., 2020). Table 1 summarizes characteristics and study variables for the baseline and follow-up study participants included in the present analyses.

Potential volunteers for PIP were screened by phone and again by an in-person medical history interview. Excluded from participating were people who endorsed: a history of cardiovascular or cerebrovascular disease (including treatment for or diagnoses of hypertension, stroke, myocardial infarction, congestive heart failure, and arrhythmias); history of any chronic medical or neurological disorder (including type 1 and type 2 diabetes, emphysema, rheumatologic conditions, seizure disorders, and chronic hepatitis); prior neurosurgery; current treatment for or self-reported psychiatric conditions; consuming alcohol equaling or exceeding 5 servings 3 or more times per week; regular use over-the-counter or prescribed medications with autonomic, cardiovascular, or neuroendocrine effects (e.g., beta-blockers, decongestants, corticosteroid inhalers); regular use of psychotropic medications; history of metal exposure or presence of metallic implants unsafe for MRI; color-blindness; self-reported claustrophobia; and, for women, pregnancy (as verified by urine test). These exclusion criteria were used to limit the influence of medications and chronic illnesses on measures of subclinical disease status. Participants were compensated $175.00 US for completing baseline study visits and $87.50 US for the follow-up study visit. Informed consent was obtained from all participants, and approval was granted by the University of Pittsburgh Human Research Protection Office (Protocol number: 07110287). Dates of data collection for the full PIP cohort spanned from August 2008, to July 2017.

Overview of Study Design and Measures

At the time of initial testing, PIP participants attended multiple study visits. These entailed (a) informed consent; (b) medical and demographic interviews; (c) anthropometric assessments of height, weight, and body composition; (d) seated measurement of blood pressure; (e) completion of questionnaires to assess health behaviors and psychosocial characteristics; (f) carotid artery ultrasonography; (g) fasting phlebotomy; and (h) a magnetic resonance imaging (MRI) protocol. Participants were instructed to fast for 8 h prior to a single initial study visit, which involved fasting phlebotomy, a light meal, and then MRI testing. This visit was scheduled to occur between 7:00AM and 11:00AM for all participants.

In September of 2011, an fMRI task involving viewing and reappraising unpleasant scenes from the International Affective Picture System (Lang et al., 2008) was added to the MRI visit of the PIP study. A total of 176 participants completed this fMRI task. For these participants, a median of 55 days separated the MRI and ultrasonography visits at initial (baseline) testing (range = 2 to 175 days). Of the latter 176 participants, 146 returned for a follow-up carotid artery ultrasound assessment that included fasting phlebotomy and the re-assessment of medical status and other measures assessed at baseline (83% retention rate, median follow-up interval between the 2 carotid ultrasonography visits = 2.78 years, absolute follow-up minimum = 1.67 years and maximum = 5.02 years). No MRI testing was conducted at follow-up. The entire span of data collection for this sub-sample of the PIP cohort began in September 2011, and ended in July 2017. The present study is the first to report on baseline fMRI measures of reappraisal and the longitudinal change in CA-IMT in the PIP cohort.

Assessment of Demographics and Health Behaviors

At the time of initial testing, demographic information was collected to assess age, race and ethnicity, income, and education (years of schooling). At that time and again at follow-up, participants reported on their smoking status and frequency of alcohol consumption over the past week. Biological sex assigned by a physician at birth was self-reported.

Assessment of Conventional Cardiovascular Risk Factors

At the time of initial testing and again at follow-up, participants underwent assessments of seated resting blood pressure, waist circumference, and body mass index, as well as fasting glucose and lipid levels. As detailed previously (Gianaros et al., 2017), seated resting blood pressures (BPs) were obtained using an oscillometric method, wherein a total of 3 BPs were taken 2 min apart after an acclimation period, with the

Table 1 Demographic information and descriptive statistics for participants with and without follow-up data

Characteristics	Full sample (N =176)	Follow-up (N = 145)
Women (%)	50.6	53.4
Age (years)	40.1 ± 6.3	40.4 ± 6.1
Race and ethnicity (%)		
White	68.8	71.0
Black/African American	26.1	25.5
Asian/Asian American	4.0	2.1
Multiracial	0.6	0.7
Other	0.6	0.7
Number of school years completed	16.3 ± 3.3	16.3 ± 3.2
Smoking status (%)		
Never smoked	61.4	66.2
Former smoker	19.9	19.3
Current smoker	18.8	14.5
Number of drinks in the last week	3.1 ± 4.6	3.0 ± 4.2
Body mass index (kg/m^2)	26.7 ± 5.2	26.8 ± 5.5
Waist circumference (in)	35.2 ± 5.5	35.4 ± 5.6
Total cholesterol (mg/dL)	183 ± 33.9	184 ± 33.0
Triglycerides (mg/dL)	95.7± 56.3	95.2 ± 59.0
HDL (mg/dL)	51.8 ± 15.8	51.7 ± 13.6
LDL (mg/dL)	113.0 ± 27.7	114.0 ± 28.0
Glucose (mg/dL)	88.6 ± 8.6	88.9 ± 8.7
Systolic blood pressure (mmHg)	120.0 ± 11.4	120.0 ± 11.7
Diastolic blood pressure (mmHg)	71.0 ± 9.5	71.2 ± 9.4
Heart rate (bpm)	77.4 ± 11.6	77.4 ± 11.2
Framingham 10-year risk score (%)	1.1 ± 2.1	1.2 ± 2.2
“Look Neutral” rating (1–5)	1.3, 95% CI [1.2, 1.3]	1.2, 95% CI [1.2, 1.3]
“Look Negative” rating (1–5)	3.6, 95% CI [3.5, 3.7]	3.7, 95% CI [3.6, 3.7]
“Regulate Negative” rating (1–5)	3.1, 95% CI [3.0, 3.2]	3.1, 95% CI [3.0, 3.2]
“Look Negative” – “Look Neutral”	2.4, 95% CI [2.3, 2.5]	2.4, 95% CI [2.3, 2.5]
“Regulate Negative” – “Look Negative”	− 0.5, 95% CI [− 0.6, − 0.4]	− 0.5, 95% CI [− 0.6, − 0.4]
Mean CCA IMT (mm)	0.58 ± 0.10	0.58 ± 0.10
Annual progression of mean CCA IMT (mm/yr)	-	0.0056 ± 0.0229
Annual progression of mean of the maximum IMT at site of fastest progression	-	0.0904 ± 0.117

average of the last 2 of the 3 BPs being used to compute systolic (SBP) and diastolic (DBP) blood pressures. Participants’ waist circumferences were measured at the level of the umbilicus to the nearest 1/2 centimeter at end expiration. Height was measured by a vertical-mounted stadiometer (with shoes off), and weight was measured by a digital scale. At the time of initial testing and at follow-up, a research nurse performed phlebotomy. Concentrations of total cholesterol and triglycerides were measured by a CHOL and triglyceride GPO reagent, respectively, using an enzymatic, timed-endpoint method on the SYNCHRON LX System (Beckman Coulter, Inc., Brea, California). The concentration of high-density lipoprotein (HDL) cholesterol was measured with a HDLD reagent on the SYNCHRON LX System, which uses an enzymatic, time-endpoint method to uniquely facilitate a detergent that solubilizes only the HDL lipoprotein particles (Beckman Coulter, Inc., Brea, California). Low-density lipoprotein (LDL) cholesterol concentrations were estimated by the Friedewald formula. Along with other demographic and anthropometric variables, these measures were used to derive Framingham 10-year risk scores (Grundy et al., 2001) and composite measures of cardiovascular risk (see Table 1).

Assessment of Medical Conditions and Medication Use

At the time of initial testing and again at follow-up, participants underwent medical history interviews. We determined

that over the follow-up interval: (a) one participant reported a new diagnosis of and treatment for hypertension; (b) one participant began using a lipid-lowering medication; (c) two participants began using glucose control medications; (d) three participants began using psychotropic medications; (e) two participants began using sleep medication; and (f) one participant began using weight-loss medication. Out of the 89 women tested at baseline, 3 underwent hysterectomy prior to initial testing; 1 was postmenopausal prior to initial testing; 5 were premenopausal at initial testing and then peri-menopausal at follow-up; 1 was peri-menopausal, both at the time of initial testing and at follow-up; and none reported using hormone therapy at initial testing or at follow-up. Given the low base rates of changes in the above conditions and factors over the follow-up interval, we did not attempt to determine the effects of such changes on primary outcome variables (CA-IMT metrics). Nor did we exclude participants from analyses based on the changes and conditions noted above.

Assessment of Carotid Artery Intima-Media Thickness by Ultrasonography

Participants underwent carotid artery ultrasonography at baseline and at follow-up. The protocol was performed by a registered vascular technologist in the laboratory of co-author EB-M. During ultrasonography, participants were supine with their heads tilted at 45°. Using an Acuson Antares scanner (Acuson-Siemens, Malvern, PA), the technologist performed scout views of the left and right carotid arteries in both the transverse and longitudinal planes. A region-of-interest encompassing the artery walls was identified for more focused B-Mode imaging of 3 carotid areas: (1) the near and far walls of the distal common carotid artery (1 cm proximal to the carotid bulb); (2) the far wall of the carotid bulb (defined as the point where the near and far walls of the common carotid are no longer parallel and extending to the flow divider); and (3) the first cm of the far wall of the internal carotid (defined distally from the edge of the flow divider). For the 3 carotid areas (common, bulb, and internal), an optimal image was digitized for later scoring with semi-automated edge detection software (Artery Measurement System; Goteborg University, Gothenburg, Sweden). The software is used to draw two lines: one along the lumen-intima interface and one along the media-adventitia interface. The distances between the line-identified interfaces were measured in 1 cm segments, generating one measurement (in mm) for each pixel in each segment (approximately 140 measurements total for averaging). For the carotid 3 areas, the average, standard deviation, minimum, and maximum measurement values were recorded. Figure 1 illustrates carotid ultrasound images obtained at baseline and again at follow-up for one study participant.

Assessment of Annualized Progression of Common Carotid Artery Intima-Media Thickness

CA-IMT is a surrogate marker of generalized preclinical atherosclerosis that predicts future (incident) clinical cardiovascular and cerebrovascular events, as well as incident plaque development (Tschiderer et al., 2020; Willeit et al., 2020). Epidemiological findings demonstrate that an absolute CA-IMT difference of 0.10 mm corresponds to a ~ 10–15% increased risk for having a future myocardial infarction and ~ 13–18% increased risk for a cerebrovascular event (Lorenz et al., 2007). Moreover, meta-analytic evidence from clinical trials measuring CA-IMT as a surrogate endpoint shows a relative risk reduction of 0.91 (95% credible interval: 0.87–0.95) for primary clinical cardiovascular outcomes associated with an intervention effect of slowing CA-IMT progression by 0.01 mm/year (Willeit et al., 2020). Importantly, carotid artery segments exhibit differential progression rates over time, and rates of progression across arterial segments do not equally predict cardiovascular outcomes (Baldassarre et al., 2013; Mackinnon et al., 2004). The majority of evidence regarding CVD risk and the progression of CA-IMT has relied on measurement of the *far walls of the common carotid artery* (Willeit et al., 2020).

In view of cumulative evidence, to minimize the influence of progression heterogeneity across segments, to account for variable length-of-follow-up intervals, and to limit multiple statistical testing, the primary and *a priori* outcome variable (dependent measure) for analysis was the annualized progression rate of mean CA-IMT from the common carotid artery, as digitized from the far wall and computed as $\text{IMT}_{\text{Time-2}} - \text{IMT}_{\text{Time-1}}$/ years of follow-up. Secondary analyses use a variable reflecting the fastest rate of progression in the mean of the maximum CA-IMT for each participant for *any* segment of the carotid arteries, as per the computational methods of prior work (Baldassarre et al., 2013). This choice of a secondary outcome measure is predicated on findings indicating that the carotid segment exhibiting the fastest progression rate of the mean of the maximum CA-IMT for a given individual may outperform other metrics in the prediction of future cardiovascular events (Baldassarre et al., 2013). CA-IMT data for one participant were excluded from analyses because of excessive movement artifacts present in the ultrasound images, yielding an analytical $N = 145$ for the machine learning analyses of CA-IMT longitudinal progression described below.

Assessment of fMRI Activity During Cognitive Reappraisal

Participants completed a reappraisal task similar to the one originally developed by Ochsner and colleagues, 2002). This task was administered as an event-related fMRI paradigm, as detailed previously (Gianaros et al., 2014). In brief,

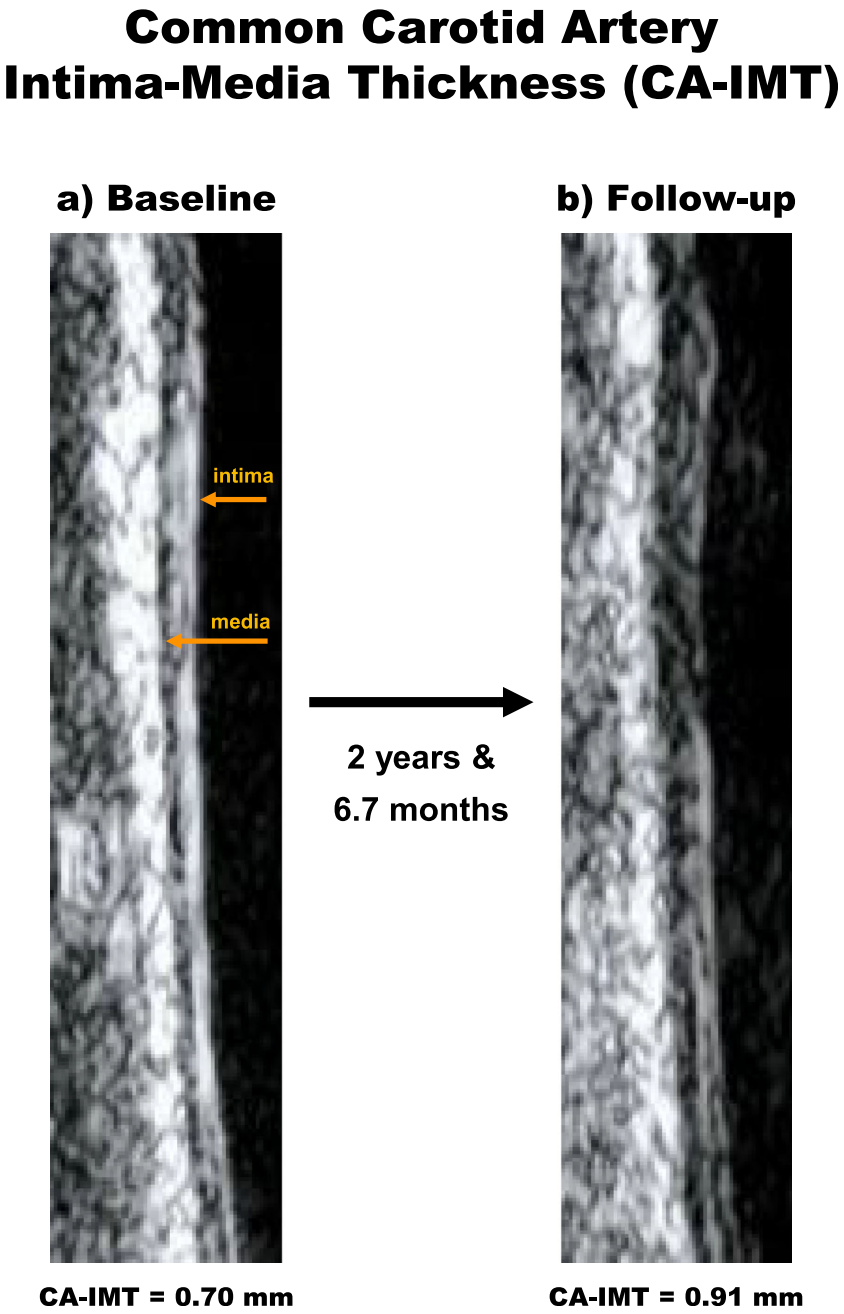

Fig. 1 Ultrasound images of the left common carotid artery (CCA) for a single participant tested at baseline (panel a) and then 2 years and 6.7 months later (panel b). This participant exhibited an annualized progression of average carotid artery intima-media thickness (CA-IMT) along the far wall of the CCA of 0.08/mm per year. The bottom of the images reflects the proximal region of the CCA and the top the distal regions of the CCA (toward the heart and head, respectively)

participants underwent a standardized training session on reappraisal and allowed time for guided practice prior to brain imaging. Participants were instructed that they would see unpleasant and neutral scenes after a cue that provided one of two instructions: "Look" and "Decrease". All scenes were drawn from the International Affective Picture System (IAPS; http://csea.phhp.ufl.edu/media.html). When cued by the "Look" instruction, participants were asked to think and feel naturally. When cued by the "Decrease" instruction, they were asked to *change* the way they thought about the scene to feel less negative (i.e., reappraise). Participants were instructed to not look away nor to think of something else, but rather to focus on each scene and actively try to change their feelings about the scene. After each scene, they used a 1-to-5 Likert-type scale to rate how negative they felt (1 = not at all; 5 = strongly negative). Thus, the task consisted of 3 conditions: "Look Neutral," "Look Negative," and "Regulate Negative," with 15 scenes per condition. Trial order was pseudo-randomized such that no more than 2 of the same cues were presented consecutively, and no more than 4 unpleasant scenes were presented consecutively. Each condition was initiated by a cue ("Look," "Decrease") for 2 s, followed by an IAPS stimulus for 7 s, and the rating scale for 4 s. Lastly, a rest screen was shown for a variable 1–3 s. Unpleasant IAPS IDs

used in the "Look Negative" condition were 2053, 2703, 3051, 3102, 3120, 3350, 3500, 3550, 6831, 9040, 9050, 9252, 9400, 9414, and 9921. Unpleasant IAPS IDs used in the "Regulate Negative" condition were 3030, 3100, 3110, 3170, 3230, 3530, 6212, 9250, 9410, 9420, 9910, 2683, 6520, 6838, and 9254**.** IAPS IDs used in the "Look Neutral" condition were: 2026, 2036, 2102, 2272, 2308, 2377, 2390, 2393, 2411, 2487, 2595, 7130, 7550, 8312, and 9210**.**

For this task paradigm, which presented IAPS stimuli in the same order across participants, there were no statistical differences in IAPS normative ratings for valence and arousal between the "Look Negative" and "Regulate Negative" conditions. IAPS stimuli for all conditions also included people (no stimuli had only inanimate objects). Lastly, there were no statistical differences in normative IAPS arousal and valence ratings between the first and second halves of the task paradigm for the conditions that were modeled for internal consistency analyses below (see additional data posted online at https://osf.io/hk6qx/).

Likert-type ratings of negative affect after each trial were used to derive 2 variables: Self-reported affective reactivity ("Look Negative" – "Look Neutral" ratings) and what has been referred to as "reappraisal success" ("Regulate Negative" – "Look Negative" ratings) as per prior fMRI studies of reappraisal (e.g., Wager et al., 2008). Study materials that include task training instructions and a post-task experimental questionnaire used to query participants about the actual emotion regulation strategies that they used during the task are available online (https://osf.io/hk6qx/). One participant among the 176 tested at baseline did not complete the post-task questionnaire because of experimenter error. This yielded an $N = 175$ for ancillary coding of whether and how participants engaged in reappraisal (see below).

MRI Data Acquisition and Preprocessing

Brain imaging was conducted using a 3-Tesla Trio TIM scanner (Siemens, Erlangen, Germany). Prior to imaging, a T1-weighted magnetization prepared rapid gradient echo (MPRAGE) structural image of the brain was obtained by these parameters: repetition time = 2,100 msec; inversion time = 1,100 msec; echo time = 3.31 msec; and flip angle = 8^0. There were 192 sagittal slices (1 mm thick, no spaces between slices) having a matrix size = 256 × 208 pixels (field-of-view [FOV] = 256 × 208 mm). Functional blood-oxygen-level-dependent (BOLD) image acquisition parameters for the IAPS task were: matrix size = 64 × 64 pixels (FOV = 205 × 205 mm), TR = 2,000 ms, TE = 28 ms, and FA = 90°. Thirty-nine slices per volume were collected along an inferior-to-superior encoding direction. Each slice was 3 mm in thickness (no gap). A 6-s countdown preceded task onset. The 3 volumes of this countdown were not modeled, nor were the 3 volumes collected after the offset of the final rest period (344 functional run volumes in total).

fMRI data for the IAPS task were preprocessed with statistical parametric mapping software (SPM12; http://www.fil.ion.ucl.ac.uk/spm). For spatial preprocessing, T1-weighted MPRAGE images were classified into 6 tissue types. Biased-corrected and deformation field maps were then computed. Functional images were realigned to the first image of the series by 6-parameter rigid-body transformation, using the re-slice step to match the first image on a voxel-by-voxel basis. Before realignment, slice-timing correction was applied to account for acquisition time variation. Realigned images were co-registered to each participant's skull-stripped and biased-corrected MPRAGE image. Co-registered images were normalized to Montreal Neurological Institute (MNI) space. Normalized images were smoothed by a 6-mm full-width-at-half-maximum (FWHM) Gaussian kernel. Preprocessed images were manually (visually) inspected to verify the absence of pipeline errors and suitability for analysis.

In within-individual fMRI analyses, univariate general linear models (GLMs) were estimated to compute contrast maps that were used for prediction analysis described below. Task events were modeled by rectangular waveforms convolved with the default hemodynamic response function in SPM12. These regressors modeled events of the trial (i.e. cue, IAPS scene, rating period, rest) specific to each condition (12 task regressors in total). In each GLM, the six realignment parameters from pre-processing were included as nuisance regressors, and low-frequency artifacts were removed by a high-pass filter (128 s). Error variance was estimated and then weighted by restricted maximum likelihood estimation, as implemented in the robust weighted least squares (WLS) toolbox, v4.0 (Diedrichsen & Shadmehr, 2005). Linear contrasts were computed as "Look Negative vs. Look Neutral" and "Regulate Negative vs. Look Negative" comparisons corresponding to the IAPS scene viewing periods. Main effects corresponding to the latter contrasts are determined from individual GLMs at the group (between-individual) level with whole-brain correction for multiple testing using a voxel-wise and false discovery rate (FDR; Benjamini & Hochberg, 1995) threshold of 0.05 for display purposes in Figure 2.

Statistical Analyses

As preregistered, two primary research questions were addressed: The first was whether individual differences in brain activity during the *viewing* of unpleasant relative to neutral IAPS scenes predicted the multiyear change in CA-IMT (in mm per year). The second was whether individual differences in brain activity during the *reappraisal* vs. the viewing of unpleasant IAPS scenes predicted the multiyear change in CA-IMT. We expected that multivariate and whole-brain

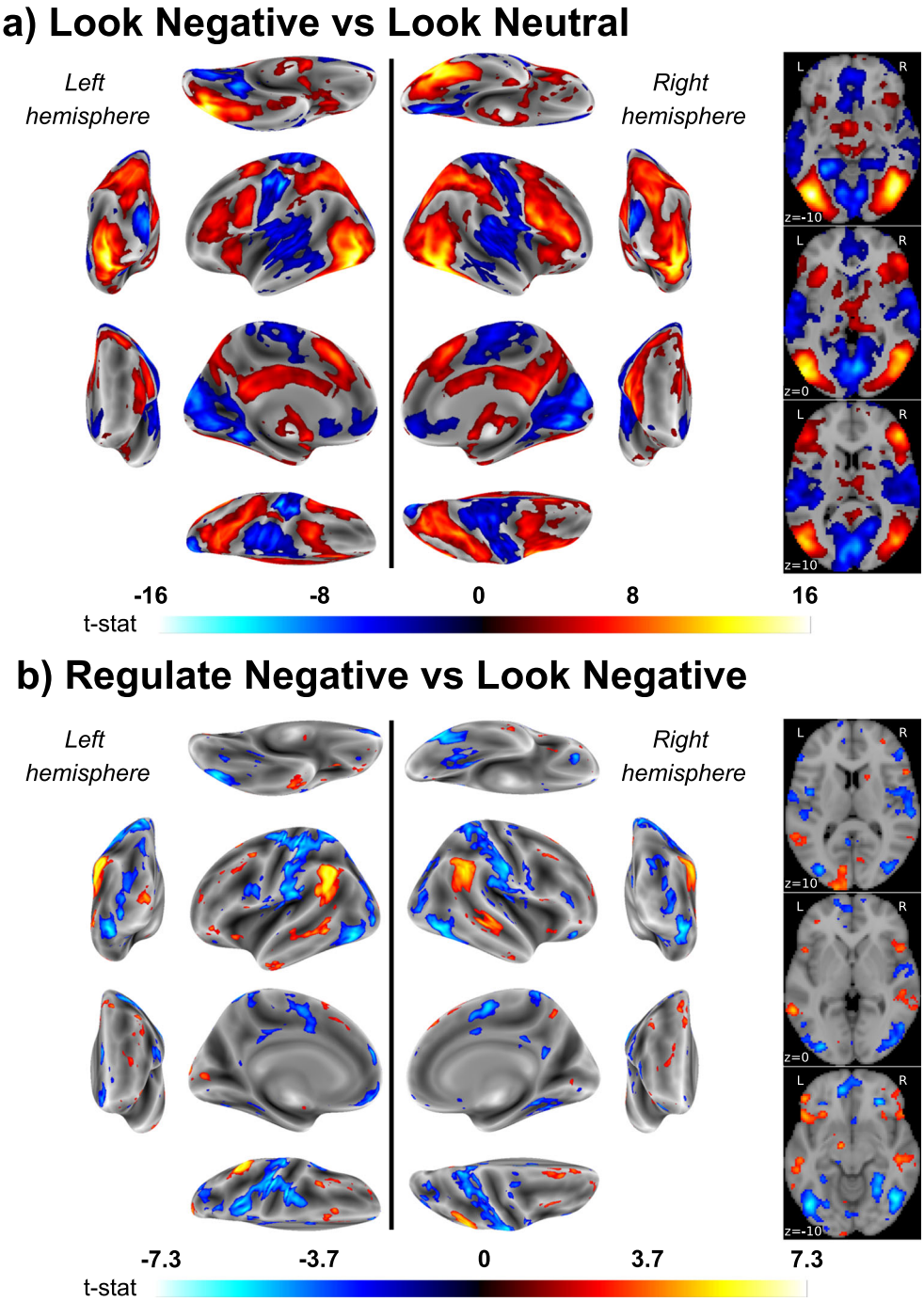

Fig. 2 Color-scaled T-maps of brain areas exhibiting significant BOLD signal changes for the contrasts of (A) "Look Negative vs. Look Neutral" trials and (B) "Regulate Negative vs. Look Negative" trials. Maps in A–B correspond to statistical parametric T-maps and are shown at a false discovery rate (FDR) threshold of 0.05. On the left, map values are projected on the lateral, medial, dorsal, ventral, anterior and posterior brain surfaces for both hemispheres. On the right, axial planes are depicted for to z coordinates of − 10, 0 and 10. Warmer colors (red-orange) reflect relative increases in activity, whereas cooler colors (blue) reflect relative decreases

patterns evoked by viewing (question 1) and reappraising (question 2) unpleasant IAPS scenes would predict the annualized rate of progression of (a) far-wall CA-IMT in the common carotid (primary study dependent measure) and (b) the mean of the maximum CA-IMT in the carotid segment exhibiting the fastest rate of progression for a given individual (secondary study dependent measure).

The independent variable used for the first question was the whole-brain fMRI contrast map corresponding to the "Look Negative vs. Look Neutral" comparison. The independent variable used for the second question was the whole-brain fMRI contrast map corresponding to the "Regulate Negative vs. Look Negative" comparison. For all analyses using whole-brain fMRI contrasts maps, we applied a mask that included only gray matter voxels. This operation was performed using the function, "masking.apply_mask," which is available in nilearn (Abraham et al., 2014). As noted, the primary dependent variable used for both study questions was

operationalized as the annualized progression of mean CA-IMT from the far wall *of the common carotid artery*, as computed by the change in mm per year. The secondary dependent variable used for both study questions was operationalized as the annualized progression of the mean of the maximum CA-IMT of the carotid artery segment showing the fastest progression for a given person, computed as mm change per year following computational steps detailed previously (Baldassarre et al., 2013).

To establish generalizability in all statistical models testing predictive associations for both primary study questions and all independent and dependent variables, nested and k-fold cross-validation was implemented to (a) optimize regression estimators in an "inner loop" and then (b) determine predictive generalizability in an "outer loop" using leave-one-out cross-validation. Specifically, machine learning analyses with regularization (penalization) and feature selection were executed in a LASSO-PCR framework (Kohoutova et al., 2020).

In LASSO-PCR, principal components dimensionality reduction of the voxel-wise predictor space of the contrast maps for the "Look Negative vs. Look Neutral" (question 1) and "Regulate Negative vs. Look Negative" (question 2) comparisons was followed by optimizing the penalty parameter, λ, in an inner loop applying 5-fold cross-validation. In this way, participants were divided into training (80%) and testing (20%) samples by stratifying over each CA-IMT outcome variable distribution for primary and secondary analyses. Within each cross-validation fold, LASSO was conducted on training samples using a sequence of 1,000 λ values, and the performance of each λ was determined by calculating the mean squared error (MSE) between predicted and observed outcome variables in respective testing (hold-out) samples. After identifying the optimal λ across all test samples, the entire LASSO procedure was repeated using optimal λs on the entire sample to produce a predictive model.

To test the generalizability of the LASSO models and to generate estimates of predicted outcomes for each participant, we repeated the above process in an outer cross-validation loop using the leave-one-out method. The final predictive performance of a given LASSO model was summarized by concatenating across the outer loops. Here, relationships between predicted and observed values were summarized by Pearson correlation coefficients and corresponding 95% bootstrapped confidence intervals (CIs). The discrepancy between predicted and observed values was calculated by the mean absolute error (MAE). Following guidelines for predictive modeling, variance in observed values explained by predicted values (R^2) was calculated by the sums-of-squares formulation (Poldrack et al., 2020). Bayes factors BF10 and BF01 were computed using the 'BayesFactors' package (v0.9.12–4.2; Morey & Rouder, 2011) to estimate the statistical evidence of prediction effects, complementing the information provided by conventional p-values (Wagenmakers, 2007). BF10 reflects the posterior probability of the alternative hypothesis, relative to the null, whereas BF01 reflects its inverse—corresponding to statistical evidence for the null relative to the alternative hypothesis. For any outcome where generalization to unseen (test) data was observed (i.e., leave-one-out $R^2 > 0$), a final predictive map was generated by extracting the feature weights after fitting the LASSO-PCR to the entire dataset. This map was further multiplied by the input data covariance matrix to facilitate appropriate interpretation of the weights with respect to the response variable (Haufe et al., 2014). Likewise, any individual features that reliably contributed to observed predictive associations were planned *a priori* to be estimated by bootstrap resampling (5,000 resamples) at $p < 0.05$.

Ancillary Analyses

As contingent on any observed findings derived from the first and second study questions above, statistical tests were planned (preregistered) to evaluate whether conventional measures of CVD risk modified associations between multivariate brain patterns and the progression of CA-IMT. These included contingent multiple regression tests of whether Framingham risk scores at the time of initial (baseline) testing would moderate predicted vs. observed CA-IMT associations. If moderation by Framingham scores was observed, then further sensitivity testing was planned. Here, age, sex, and smoking status were planned to be removed from Framingham risk scores to compute a composite cardiometabolic risk score by z-scoring and averaging components of the metabolic syndrome; namely blood pressure, waist circumference, body mass index, lipid levels, and glucose. Collectively, using Framingham and composite cardiometabolic risk scores as effect modifiers would address questions about the degree to which affective brain patterns may interact with conventional CVD risk factors to predict CA-IMT progression. In addition to plans to test for effect modification by conventional CVD risk factors, additional ancillary testing was planned to evaluate whether self-reports of negative affect evoked by viewing or reappraising unpleasant IAPS scenes (a) correlated with the progression of CA-IMT, and if so, (b) modified the predictive associations between multivariate brain patterns and CA-IMT progression.

In final ancillary testing, we computed the within-session reliability of fMRI activity evoked by the task paradigm (i.e., internal consistency computed by the intraclass correlation coefficient; ICC) following similar steps used previously (Gianaros et al., 2020). Specifically, GLM analyses were used to generate fMRI contrast maps for the approximate first and second halves of the IAPS task paradigm (i.e., the first 23 and last 22 trials). ICC analyses were then conducted by

calculating the correlation between contrast maps from the first and second halves of the task and applying the Spearman-Brown (SB) correction method on a voxel-wise basis. Comparable analyses were executed for self-reports of negative affect.

As contingent on findings from the first and second study questions, we further planned to estimate the ICCs of the final predictive weight maps for CA-IMT generated by LASSO-PCR. Here, the approach was to compute the dot-product of all of the pairs of contrast maps generated by the split-half procedure described above. For all within-session reliability testing, we planned to adopt a conservative approach that would estimate out-of-sample ICCs. The basis for this approach is that evaluating within-session reliabilities on the same individuals used to generate predictive weight maps may over-estimate ICC values. Accordingly, we planned to embed these calculations within the cross-validation procedures that assessed the generalizability of the LASSO-PCR models. In this way, the whole-brain predictive patterns estimated in each training set of the outer fold in cross-validation could be used to produce a dot-product with the pair of split-half contrast maps of the individual's data used for testing. Final ICC values were planned to be calculated between the out-of-sample dot-products of each split-half contrast map concatenated across all participants.

Assessment of Task Comprehension

We explored the possibility that excluding those individuals who failed to engage in reappraisal during the fMRI task could alter (e.g., improve) associations between predicted vs. observed annualized CA-IMT values. To this end, two of the authors (PJG and CD) independently coded free-response descriptions of the emotion regulation strategies that participants used during the fMRI task as reflecting reappraisal or not (binary variable: 0 = no, 1 = yes). Inter-rater agreement was computed by the two-way random effects ICC method to determine absolute inter-rater agreement (Koo & Li, 2016). Discrepancies between coders were first adjudicated by conversation. Unresolved judgments were adjudicated by a third rater who was blinded to prior coding (co-author, KM) before sensitivity tests reported below. To these ends, participants were asked to describe the primary and any secondary strategies they used to decrease their emotional responses to the unpleasant IAPS scenes in the "decrease" (i.e., "Regulate Negative") condition. Specifically, they were asked: "What sorts of things did you tell yourself to try to help you feel differently in response to the negative pictures?" The response format was open ended.

Coding of participant responses followed methods detailed previously (McRae, Ciesielski, & Gross, 2012). Specifically, responses were coded as reflecting reappraisal if falling into any of following categories: (1) explicitly positive, (2) change in current circumstances, (3) reality challenge, (3) change of future consequences, (4) ascribing agency to a person capable of changing the circumstances depicted in the scene, (5) distancing, (6) problem-solving, (7) acceptance, and (8) non-specific reappraisal. Failures to reappraise (e.g., avoiding looking at or thinking about the IAPS stimulus, using expressive suppression as the primary strategy, or using a strategy that is not cognitive) resulted in a score of 0. As noted, 1 participant did not complete the post-fMRI inventory. There were 8 participants who were judged as failing to use reappraisal by the primary raters. An additional 2 participants were judged as failing to use reappraisal after adjudication by the third rater. There were 3 additional participants who provided responses that could not be judged by the raters as reflecting reappraisal or not. Inter-rater agreement for coding primary strategies as reappraisal was ICC = 0.74; 95% CI = 0.66–0.80, and that for secondary strategies was ICC = 0.79; 95% CI = 0.68–0.86. Of the participants who were judged as not engaging in reappraisal by the raters, 8 were among those with longitudinal CA-IMT data. Thus, data for these 8 participants were removed in ancillary sensitivity tests of the primary study questions.

Non-Preregistered Exploratory Analyses

In analyses that were not preregistered, we repeated the machine-learning (LASSO-PCR) modeling described above in an attempt to predict individual differences in self-reported affective reactivity ("Look Negative" – "Look Neutral" ratings) and "reappraisal success" ("Regulate Negative" – "Look Negative" ratings). These were implemented to explore whether the fMRI contrast maps that were used to model CA-IMT were sufficient for predicting variables of conceptual relevance to negative affect and reappraisal. As in tests of the primary research questions on CA-IMT, the independent variable used to predict affective reactivity was the whole-brain fMRI contrast map corresponding to the "Look Negative vs. Look Neutral" comparison. The independent variable used to predict reappraisal success was the whole-brain fMRI contrast map corresponding to the "Regulate Negative vs. Look Negative" comparison. As planned for CA-IMT analyses, we assessed the ICC of maps that predicted self-reported changes in negative affect by the cross-validation, split-half, out-of-sample, and dot-product steps above.

All machine learning and related analyses of brain imaging data were performed in Python, version 3.8, using the scikit-learn (Pedregosa et al., 2011) and nilearn (Abraham et al., 2014) libraries. Statistical analyses of non-brain imaging data

were performed in R, version 3.6.1 (R Program for Statistical Computing).

Results

Progression of CA-IMT over the Multiyear Follow-Up Period

As expected in this midlife sample of 145 adults with complete longitudinal data, far-wall common carotid CA-IMT (primary study dependent measure) exhibited a positive annualized progression over the follow-up period, with an average increase of 0.006 mm per year (95% bootstrapped CI = 0.002 to 0.01 mm per year). Likewise, the mean of the maximum CA-IMT in the carotid segment exhibiting the fastest rate of progression for a given individual (secondary study dependent measure) exhibited progression over the follow-up interval, with an average increase of 0.090 mm per year (95% bootstrapped CI = 0.074 to 0.110 mm per year). The higher progression rate for the secondary study measure is comparable to prior findings and was anticipated because the site of fastest maximum CA-IMT progression includes arterial segments likely to contain focal atherosclerotic lesions driving greater CA-IMT (Baldassarre et al., 2013).

Self-Reported Negative Affect During the fMRI Task

Among the 176 participants with complete baseline data, viewing unpleasant IAPS scenes compared with neutral scenes increased self-reported negative affect by an average of 2.38 ± 0.71 (SD) points on a 1-to-5 Likert-type scale (M = 3.64 ± 0.65 vs 1.26 ± 0.32, paired $t[175] = 44.19$, $p < 0.001$). Reappraising unpleasant IAPS scenes as compared with viewing these scenes decreased self-reported negative affect by 0.51 ± 0.62 points, M =3.14 ± 0.65 vs. M = 3.64 ± 0.65, paired $t(175) = 10.89$, $p < 0.001$. These findings were unchanged in direction and statistical significance when analyses were restricted to only those 145 participants with complete follow-up data.

Main Effects of the fMRI Task and Within-Session Reliability of Contrast Maps

Among the 176 participants with complete baseline data, the "Look Negative vs. Look Neutral" contrast revealed that viewing unpleasant IAPS scenes engaged a distributed ensemble of brain regions implicated in processing complex visual affective stimuli. Brain regions exhibiting a relative increase in activity to unpleasant IAPS scenes included the medial temporal lobe (encompassing the amygdala), as well as areas of the dorsal-medial pre-frontal, anterior cingulate, anterior insular, and visual cortices in the occipital lobe. Brain regions exhibiting a relative decrease in activity to unpleasant IAPS scenes included ventral portions of the medial prefrontal cortex and medial portions of occipital and parietal cortices, as well as regions of the pre- and post-central gyri. Figure 2 (panel a) illustrates main effects of the fMRI task (see also contrast maps available at NeuroVault (https://neurovault.org/collections/10337). There was wide variability, however, in the within-session reliability of mass univariate fMRI activity changes distributed across the brain—with only 574 voxels (0.28% of the gray matter voxels) exhibiting "good-excellent" ICC values (maximum ICC = 0.84). The median ICC value of the entire contrast mass univariate contrast map was 0.21, reflecting poor reliability (see panels a and b of Figure 3, as well as voxel-wise maps available at NeuroVault).

As illustrated in Figure 2 (panel b), the "Regulate Negative vs. Look Negative" contrast reveals that reappraising unpleasant IAPS scenes engaged a distributed ensemble of brain regions thought to be involved in the cognitive control of emotion. Brain regions exhibiting a relative increase in activity while reappraising unpleasant IAPS scenes included prefrontal areas of the middle, inferior, and superior frontal gyri, as well as the inferior parietal lobule and anterior insula. Brain regions exhibiting a relative decrease in activity while reappraising unpleasant IAPS scenes included portions of the precentral gyrus, middle and inferior frontal gyri, inferior temporal gyri, and posterior cingulate cortex. Compared to the "Look Negative vs. Look Neutral" contrast maps, there was an overall reduction of ICC values on a voxel-wise basis, suggesting less within-session reliability of reappraisal-related fMRI activity (see panels a and b of Figure 3, as well as voxel-wise maps available at NeuroVault). More precisely, just 42 voxels (0.02% of grey matter voxels) exhibited "good-excellent" ICC values (maximum ICC = 0.82). The median ICC value across all voxels for this mass univariate contrast map was 0.11, reflecting poor reliability.

For completeness of reporting and relative comparisons to fMRI activity patterns, ICCs for self-reports of negative affect ratings were as follows: "Look Neutral" = 0.57; "Look Negative" = 0.74; "Regulate Negative" = 0.73; "Look Negative - Look Neutral" = 0.71; and "Regulate Negative - Look Negative" = 0.54. Collectively, the latter findings reflect moderately higher reliabilities for self-reports of negative affect than for fMRI activity in this task paradigm.

Prediction of CA-IMT

Analyses tested whether individual differences in brain activity during the viewing of unpleasant affective scenes predicted the annualized rate of progression of (a) far-wall common CA-IMT and (b) the mean of the maximum CA-IMT in the carotid segment exhibiting the fastest rate of progression for a given individual. By cross-validated LASSO-PCR modeling, the annualized progression of far-wall common CA-IMT was

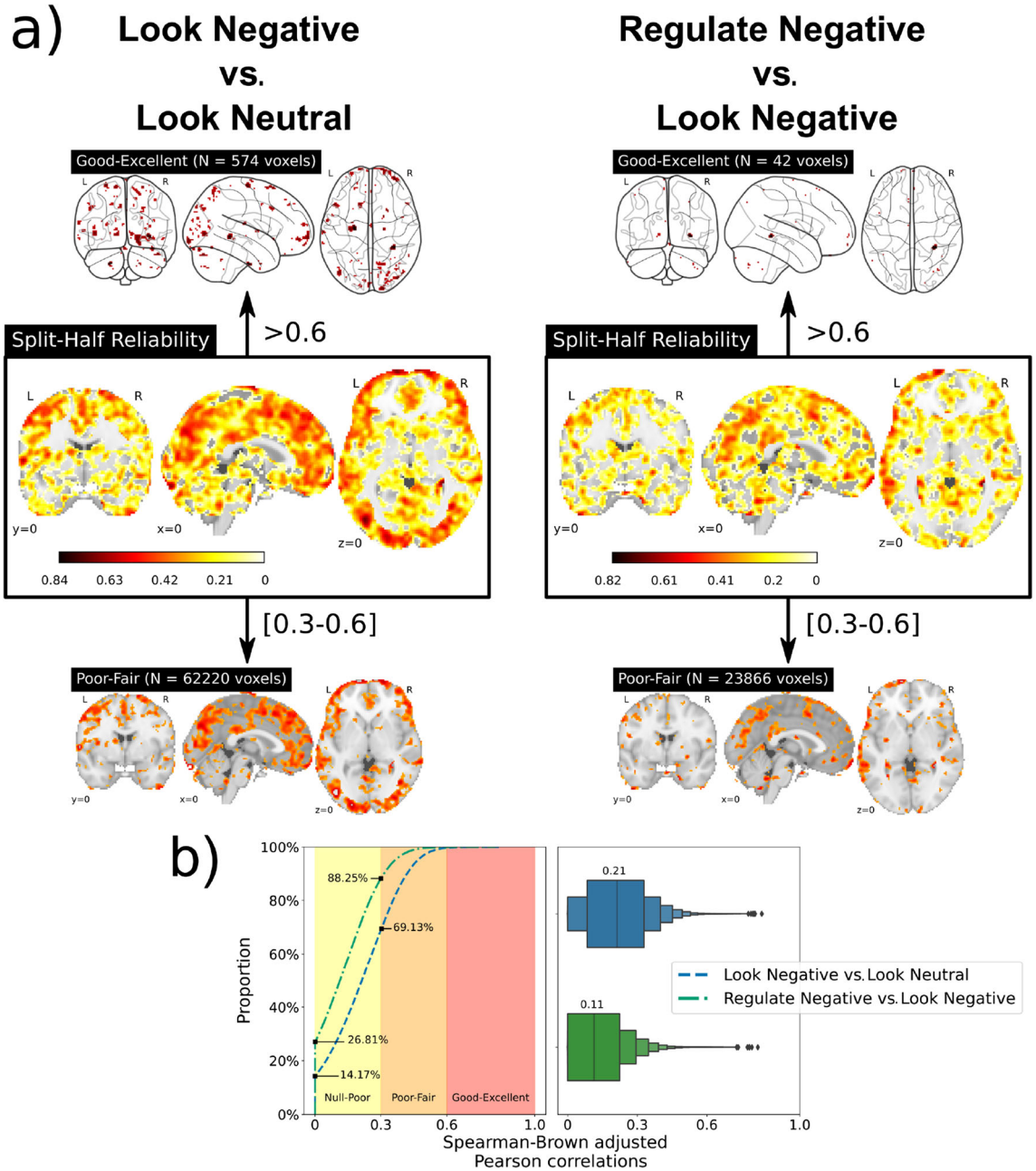

Fig. 3 (**a**) Whole-brain voxel-wise intraclass coefficient (ICC) summaries that reflect the split-half internal consistencies of the "Look Negative vs. Look Neutral" contrast maps and "Regulate Negative vs. Look Negative" contrast maps. To aid in visualizing the "good-excellent" ICC range due to the scarcity of voxels, glass brain plots were employed. (**b**) Comparison of reliabilities from both contrast maps using the empirical distribution function and box plots that reflect the median and distribution of the ICC values

not predicted by the contrast of "Look Negative vs. Look Neutral", $r(143) = -0.411$, 95% CI = − [0.939–0.353], MAE = 0.017 mm, R^2 = -0.022, BF10 = 0.031, and BF01 =32.492. The negative signs of the r and R^2 values for hold-out (test) set evaluations likely reflect the extremely poor model fits and should be interpreted as equivalent to values of zero. More precisely, apparent negative effect sizes can be attributed to the models not reliably identifying predictive principal components.

Similar observations were made for models using "Look Negative vs. Look Neutral" contrasts to predict the mean of the maximum CA-IMT in the carotid segment exhibiting the fastest rate of progression for a given individual, $r(143) = -0.139$, 95% CI = − [0.39–0.042], MAE = 0.056, $R^2 = -0.05$, BF10 = 0.075, and BF01 = 13.34.

To test whether these observed poor performances could be due to excessive shrinkage during model estimation, we repeated these calculations in sensitivity tests that were not

preregistered by replacing the LASSO regression model (a L1 regularization term) for ridge (an L2 regularization term) and elastic net (both L1 and L2 regularization terms) models. Likewise, we also tested whether the LASSO-PCR model behaved differently by changing the outer cross-validation to a 10-fold partition scheme. In all these cases, similar results were obtained insofar as no CA-IMT variable was reliably predicted by any fMRI pattern.

As above for the first study question, machine learning analyses were used to test whether individual differences in brain activity evoked by reappraising unpleasant IAPS scenes predicted the annualized rate of progression of (a) far-wall common CA-IMT and (b) the mean of the maximum CA-IMT in the carotid segment exhibiting the fastest rate of progression for a given individual. Using cross-validated LASSO-PCR, the annualized progression of far-wall common CA-IMT was not predicted by the "Regulate Negative vs. Look Negative" contrast, $r(143) = -0.367$, 95% CI = − [0464–0.270], MAE = 0.017 mm, $R^2 = -0.032$, BF10 = 0.034, and BF01 = 29.299. The Bayes factors again indicated strong evidence in favor of the null hypothesis. Similar findings were observed for models using "Regulate Negative vs. Look Negative" contrasts to predict the mean of the maximum CA-IMT in the carotid segment exhibiting the fastest rate of progression for a given individual, $r(143) = -0.405$, 95% CI = − [0.792–0.301], MAE = 0.056 mm, $R^2 = -0.048$, BF10 = 0.031, and BF01 = 32.075. As with the models for the progression of common CA-IMT, the models trained to predict the mean of the maximum CA-IMT had strong to very strong evidence in favor of the null hypothesis. Similar to findings for the "Look Negative vs. Look Neutral" maps, there were no differences in results after changing the regularization terms in the regression models and the outer cross-validation strategy.

Lastly, sensitivity testing that excluded the 8 individuals who were judged as failing to use reappraisal during the fMRI task did not alter any of the above observations. In other words, the findings did not improve when including only those individuals who unambiguously engaged in reappraisal.

In view of our inability to predict CA-IMT in any of the preregistered and unplanned analyses, there was no a priori basis to execute contingent tests of whether conventional risk factors for CVD and self-reports of negative affect modified associations between multivariate brain patterns and the progression of CA-IMT. Moreover, because all machine learning approaches failed to generate a reliable fMRI pattern that predicted CA-IMT, we were unable to test whether resulting predicted vs. observed CA-IMT associations could be moderated by additional variables. For completeness of reporting, however, univariate correlations between all study variables reported herein are depicted in Figure 4, with additional correlation results available online at OSF (https://osf.io/hk6qx/).

Prediction of Individual Differences in Task-Related Changes in Self-Reported Negative Affect

In view of the null findings bearing on CA-IMT, additional testing not in the preregistration plan was conducted to test whether we could predict self-reported affective reactivity ("Look Negative" – "Look Neutral" ratings) and reappraisal success ("Regulate Negative" – "Look Negative" ratings). Here, a predictive association was found between the out-of-sample differences in affective reactivity and changes in brain activation during viewing unpleasant vs. neutral IAPS scenes ("Look Negative vs. Look Neutral" rating differences), as revealed by a nested cross-validated LASSO-PCR (Figure 5, panel a). However, this predictive association exhibited relatively weak statistical evidence by Bayes criteria, $r(143) = 0.143$, 95% CI = [− 0.027, 0.308], one-tailed$p = 0.043$, MAE = 0.520, $R2 = 0.015$, BF10 = 1.515, and BF01 = 0.66. In this case, the final predictive model retained 8 principal components from an optimal $\lambda = 1.391$, and it had an overall ICC = 0.474. A summary of areas where increased and decreased multivariate activity patterns consistently contributed to the prediction of affective reactivity after bootstrapping is provided in Supplementary Table 1.

By comparison to the affective reactivity findings above, out-of-sample differences in self-reports of reappraisal success ("Regulate Negative vs. Look Negative" rating differences) were predicted by fMRI activity changes in a nested cross-validation LASSO-PCR model (Figure 5, panel b). This effect exhibited strong statistical evidence by Bayes criteria, $r(143) = 0.457$, 95% CI = [0.307, 0.468], one-tailed$p < 0.001$, MAE = 0.418, R2 = 0.209, BF10 > 150, and BF01 < 0.001. Deploying this predictive model revealed an optimal $\lambda = 0.023$, which retained 137 principal components, yielding a whole-brain weight map with an ICC = 0.390. Repeating these analyses to exclude those 8 individuals who were judged as failing to reappraise during the fMRI task produced comparable results $r(133) = 0.415$, 95% CI = [0.239, 0.561], one-tailed $p < 0.001$, MAE = 0.421, $R2 = 0.172$, BF10 > 150, and BF01 < 0.001. A summary of areas where increased and decreased multivariate activity patterns consistently contributed to the prediction of reappraisal success after bootstrapping is provided in Supplementary Table 2.

Discussion

Does cognitive reappraisal evoke a pattern of brain activity that reliably predicts the multiyear progression of a vascular

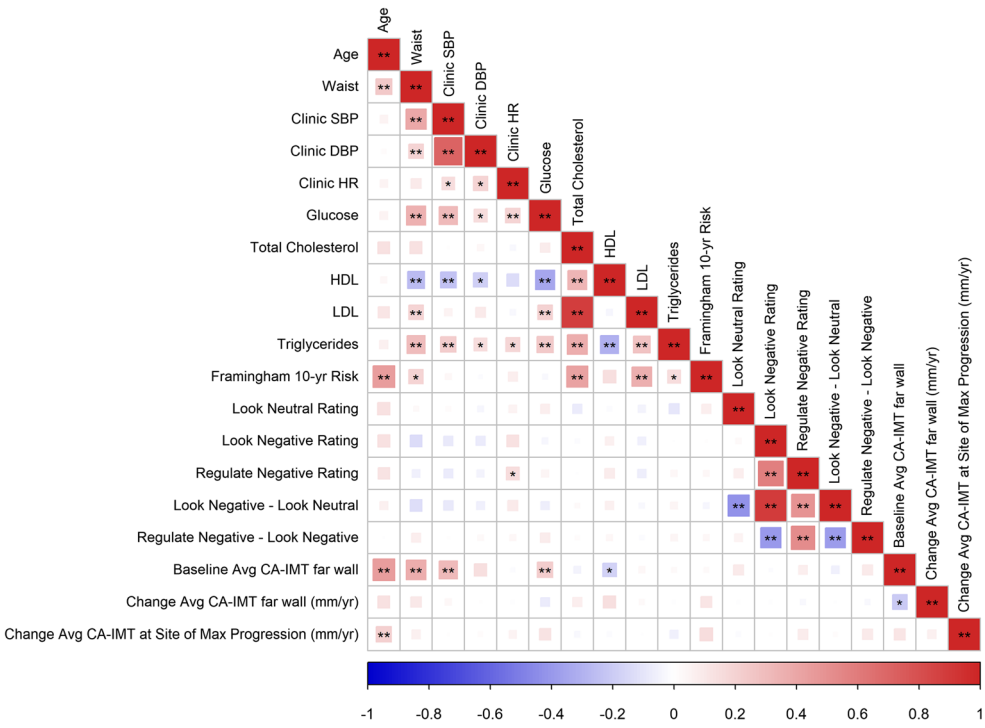

Fig. 4 A correlogram of study variables depicting the strength of their associations. Colors and sizes of each area in the correlogram correspond to the direction and size of each correlation, as coded along the scale of the horizontal axis. SBP, systolic blood pressure; DBP, diastolic blood pressure; HR, heart rate; HDL, high-density lipoproteins; LDL, low-density lipoproteins, CA-IMT, carotid artery intima media thickness; mm, millimeter. *$p < .05$; **$p < .01$

marker of cardiovascular risk among midlife individuals? Findings from the present study suggest not. Hence, viewing and reappraising unpleasant scenes engaged an ensemble of brain systems that are implicated in affective stimulus processing and the cognitive control of emotion among 176 otherwise healthy midlife individuals (Figure 2). Viewing and reappraising unpleasant scenes likewise resulted in increases and decreases in self-reported negative affect, respectively (Table 1). Notwithstanding, brain activity patterns and corresponding changes in self-reported negative affect evoked by viewing and reappraising unpleasant affective scenes did not reliably associate with the annualized change in multiple vascular markers of cardiovascular risk obtained from different segments of the carotid artery over a multiyear follow-up period among 145 individuals with complete follow-up data. Collectively, these longitudinal findings do not support hypotheses derived from prior epidemiological, psychophysiological, and neuroimaging evidence suggesting that brain activity patterns evoked by cognitive reappraisal may comprise affective neural correlates of future (prospective) changes in cardiovascular risk. Plausible explanations of the present observations could include psychometric limitations and other features of the fMRI reappraisal task; low statistical power; a short follow-up period for the assessment of carotid artery markers, as compared with prior epidemiological studies; the restricted range of preclinical and clinical disease in this otherwise healthy sample; and, lastly, heterogeneity of specific reappraisal tactics used across study participants that may obscure meaningful individual differences in the affective neural correlates of cardiovascular risk.

In line with prior epidemiological findings, CA-IMT visualized from the far wall of the common carotid artery progressed at a mean annualized rate of 0.006 mm per year among the 145 participants who returned for follow-up assessments. As expected, the mean of the maximum CA-IMT in the carotid segment exhibiting the fastest rate of progression for a given individual was appreciably higher, with an average increase of 0.090 mm per year over the follow-up interval. The latter rates of progression approximate those observed among otherwise healthy midlife adults, with rates of progression being accelerated among clinical populations and those at high risk for CVD (Willeit et al., 2020). However, we note that the progression rates of the present study sample are somewhat less than what has been observed in other midlife community-dwelling adults. For example, Kozakova et al. (2013) reported 3-year progression rates of 0.017 mm per year for men and 0.021 for women in the common carotid artery (mean ages of 44 years at baseline). It is thus possible that our exclusion criteria resulted in a sample of people for whom the average and range of CA-IMT progression are restricted. Notably, the annualized change in CA-IMT has not been consistently associated with known or emerging CVD risk factors that are assessed only at baseline. For example, in a midlife sample of nearly 16,000 adults, only small effect sizes were observed for a limited set of baseline risk factors in the prediction of the rate of change in CA-IMT, including type 2 diabetes, smoking status, HDL levels, pulse pressure (i.e., the difference between SBP and DBP), white blood cell count, and fibrinogen levels (Chambless et al., 2002). Among over 3,000 adults from the Multi-Ethnic Study of Atherosclerosis,

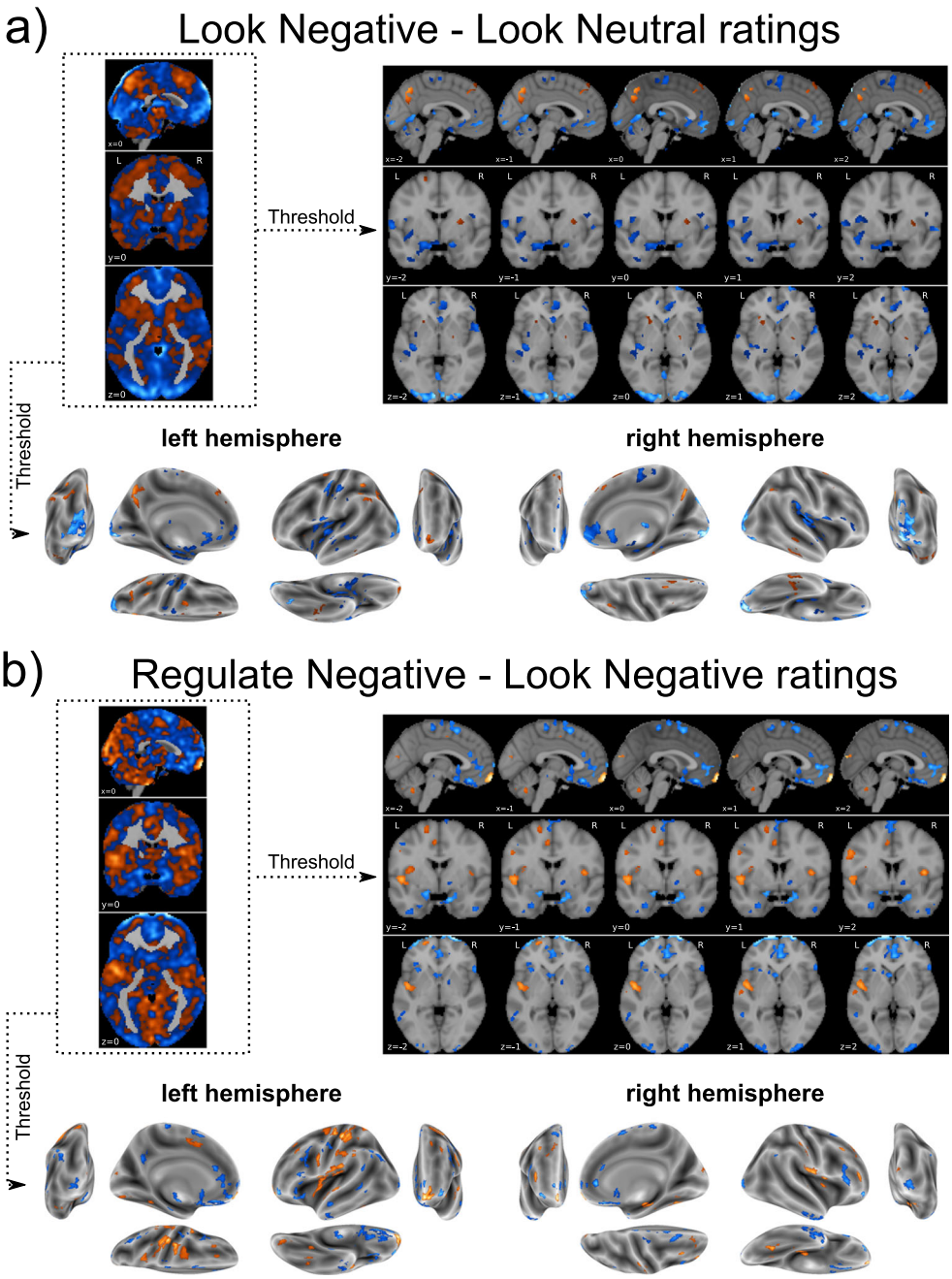

Fig. 5 Raw and thresholded weight maps used to predict individual differences in self-reported affective reactivity ("Look Negative" – "Look Neutral" ratings) and "reappraisal success" ("Regulate Negative" – "Look Negative" ratings). For thresholding, cut-offs were $p < 0.05$ via bootstrapping (5000 iterations) and cluster-extent of $k > 50$ contiguous voxels. Warmer colors (orange/yellow) reflect positive pattern weights and cooler colors (blue) reflect negative weights

only ethnicity, HDL levels, and use of medications to lower lipids and blood pressure at baseline exhibited small effect sizes correlating with the rate of change in CA-IMT in over a decade of follow-up (Tattersall et al., 2014). Thus, in the broader context of epidemiological findings and what has been observed previously for baseline predictors of the change in CA-IMT, it may be that the affective neural correlates of future changes in cardiovascular risk—if existent—are minimal in their effect sizes and unreliably detected in small samples of otherwise healthy adults who are followed over relatively brief time periods and exhibit a restricted range of progression rates. Indeed, only increased age correlated significantly with an accelerated increase in the mean of the maximum CA-IMT in the site of fastest progression the present sample, with all other baseline factors exhibiting non-statistically significant associations with longitudinal changes in CA-IMT (see Figure 4).

In extension of the above interpretive issues, as shown in Figure 3, the mass univariate patterns of brain activity evoked by viewing and reappraising unpleasant affective scenes did not exhibit particularly strong overall within-session reliabilities (cf., Berboth et al., 2021). The latter may have undermined the ability of fMRI contrast maps to predict small changes in CA-IMT over the follow-up period across

individuals (Elliott et al., 2020). Thus, it may be other baseline indicators of brain activity, such as resting state metabolism or multivariate connectivity metrics reflecting network dynamics, could be more likely to exhibit larger or more consistent patterns of association with clinically relevant CVD outcomes or intermediate risk factors (cf., Tawakol et al., 2017), possibly owing to their more suitable psychometric properties for studies of individual differences (Elliott et al., 2020; Kragel et al., 2021).

The present null findings regarding the prediction of CA-IMT can also be interpreted in the context of the heterogeneity that participants reported in the use of primary and secondary reappraisals. While cognitive reappraisal can be considered as a process to change the meaning that is ascribed to stimuli, events, and contexts to change affective experiences (Gross, 2014) or as a recategorization process that alters the construction of affective states (Barrett, 2017), there are different tactics that individuals may use to reappraise at any given time (McRae, Ciesielski, & Gross, 2012). Hence, while approximately 7.4% of the entire baseline sample was judged as failing to comply with reappraisal instructions, the remaining sample reported using a broad range of tactics to reappraise. The 4 most frequently reported *primary* strategies were coded as reality challenges (e.g., "This picture is from a movie," $N = 44$), changing the construal of future consequences ("This situation will improve with time," $N = 43$), changing the construal of current circumstances ("The person is lucky to be alive," $N = 30$), and ascribing agency to people in the affective scenes ("Professionals will help this person out of the situation," $N = 20$). Other coded reappraisal tactics were approximately equally distributed across the sample. Thus, although averaged self-reported ratings of negative affect decreased on reappraisal trials and although individual differences in these changes were moderately predicted by fMRI activity changes ($R^2 = 0.21$, Figure 5, panel b, Supplementary Tables 1–2), it is possible that between-individual variation in specific reappraisal tactics are not fully encoded in the fMRI contrast maps used to predict putative reappraisal-related health outcomes, including CA-IMT progression. That is, although cognitive reappraisal appeared to elicit "robust" effects on brain activity (Figure 2), the failure to have captured substantive between-individual variation in diverse reappraisal processes and their neural correlates in predictive modeling may have further contributed to the observed low internal consistency values of the contrast maps as compared to those for self-reported negative affect across the paradigm (e.g., Infantolino et al., 2018) and the overall patterns of null findings for CA-IMT. The latter interpretation is on par with cumulative evidence that common fMRI task paradigms and metrics, such as those used here, may have limited statistical reliability to estimate stable individual differences (Elliott et al., 2021). Moreover, post-hoc exploratory analyses not in the preregistration plan bearing on the latter point suggest the possibility that reappraisal success actually declined on average from the first to the second half of the task paradigm (Cohen's d = 0.355; see Figure 6). As shown, there was thus an increase in negative affect for reappraisal ("Regulate Negative") trials over the course of the task. By comparison, there were no statistical changes in ratings across the task for reactivity ("Look Negative") trials. Lastly, there appeared to be marked heterogeneity in changes in affective ratings for reappraisal trials (see Figure 6). In aggregate, it is thus possible that the internal consistency or reliability of fMRI contrasts maps for reappraisal is constrained both by the moderate reliability of affective performance (i.e., "Regulate Negative - Look Negative" rating difference ICC = 0.54), as well as a mean decline in overall reappraisal success over time that is variably seen across participants.

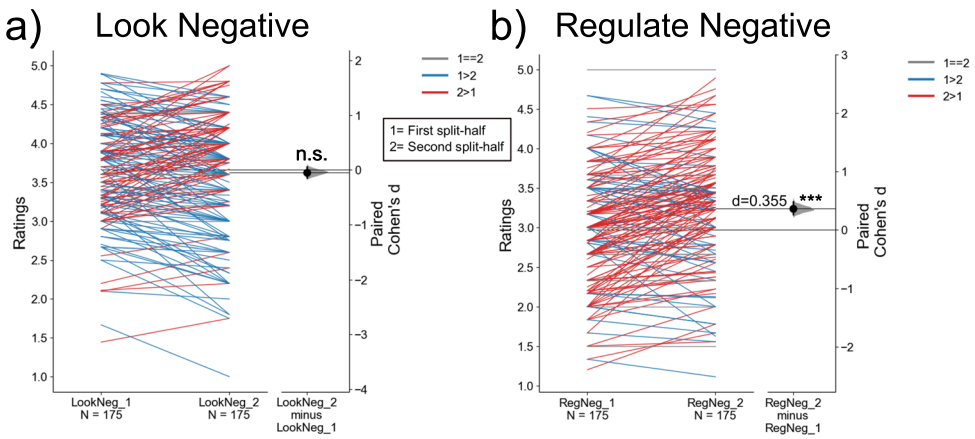

Fig. 6 A slope graph showing changes in average ratings of self-reported negative affect per person between each half of the task paradigm for the "Look Negative" (panel a) and "Regulate Negative" (panel b) conditions. Greater ratings in the first half compared with the second half are displayed with a blue line, whereas greater ratings in the second half compared with the first half are displayed with a red line. Grey lines represent no change in average ratings between halves. Changes across participants were tested by a paired *t*-test, and the size of this effect was computed as a Cohen's d for paired samples

A final interpretive consideration is that prior epidemiological work on individual differences in reappraisal and risk factors for CVD have largely focused on *trait* dimensions of emotion regulation, as often assessed by the Emotion Regulation Questionnaire (Gross & John, 2003). The present study employed an fMRI task paradigm that involved instructed reappraisal, and the correspondence between fMRI and self-report variables from this task paradigm to trait dimensions of reappraisal appears to be moderate at best (McRae, Jacobs, et al., 2012). Indeed, the ability to effectively implement reappraisal during the fMRI task paradigm may not uniformly represent or reliably index the habitual use of this emotion regulation strategy in real-world contexts. Moreover, recent evidence suggests that the habitual use of reappraisal in everyday life may moderate the effects of instructed reappraisal on cardiovascular and neuroendocrine parameters of physiology during laboratory stress testing (Jentsch & Wolf, 2020), but evidence for such moderation appears to be mixed (Griffin & Howard, 2021). In these regards, an inferential consideration is that the study exclusion criteria may have restricted the sample to those without affective disorders, which may have further constrained variability not only in CA-IMT, but also trait and state features of emotion regulation of relevance to CVD risk. There is thus a rationale for future lines of inquiry on interactions between instructed and trait features of reappraisal in the prediction of CVD risk among more diverse populations.

To close, the present findings do not indicate that multivariate brain activity patterns evoked by viewing and reappraising unpleasant scenes reliably predict the multiyear progression of a vascular marker of CVD risk (CA-IMT) among otherwise healthy midlife adults, even though individual differences in self-reported changes in negative affect were moderately predicted by such patterns. The present null findings also do not agree with those of our prior cross-sectional report on CA-IMT and fMRI activity measured during the viewing and reappraising of unpleasant scenes among 157 adults (Gianaros et al., 2014). Open questions include whether the present null findings could be attributed to the relatively small sample of adults tested and small effect sizes to be detected at the population level; the known inconsistency of baseline individual-difference factors to predict CA-IMT over relatively short and variable follow-up periods; the overall weak-to-moderate within-session reliability of brain activity patterns evoked by the fMRI task paradigm; heterogeneity in when, how, and by whom reappraisal is used to change affective states; and, the yet-to-be clarified interplay of instructed vs. trait dimensions of reappraisal in the context of CVD risk.

Additional Information

Funding Research reported in this publication was supported by the National Heart, Lung, and Blood Institute of the National Institutes of Health under Award Numbers P01 HL040962 and R01 HL 1089850. The content is solely the responsibility of the authors and does not necessarily represent the official views of the National Institutes of Health.

Data availability Data and code are publicly available at OSF (https://osf.io/hk6qx/), GitHub (https://github.com/CoAxLab/reappraisal-imt-progression), and NeuroVault (https://neurovault.org/collections/10337).

Conflict of Interest The authors declare no competing interests.

Supplementary Information The online version contains supplementary material available at https://doi.org/10.1007/s42761-021-00098-y.

Author Contribution P.J. Gianaros conceived the study and hypotheses, obtained research funding from NIH, planned the project, and oversaw data collection. E. Barinas-Mitchell oversaw the carotid artery ultrasound protocol, as well as scoring and quality control procedures to generate intima-media thickness data. P.J. Gianaros, T.E. Kraynak, C.M. DuPont, J. Rasero, J.J. Gross, K.M. McRae, A.G.C. Wright, T.D. Verstynen, and E. Barinas-Mitchell collaborated on and finalized the pre-registration and data-analysis plan. J. Rasero and T.E. Kraynak prepared and implemented machine learning models of MRI data with P.J. Gianaros and T.D. Verstynen. C.M. DuPont and P.J. Gianaros prepared and implemented regression and correlation analyses. P.J. Gianaros, T.E. Kraynak, C.M. DuPont, J. Rasero, J.J. Gross, K.M. McRae, A.G.C. Wright, T.D. Verstynen, and E. Barinas-Mitchell discussed and interpreted results, contributed to manuscript preparation and its revisions.

References

Abraham, A., Pedregosa, F., Eickenberg, M., Gervais, P., Mueller, A., Kossaifi, J., Gramfort, A., Thirion, B., & Varoquaux, G. (2014). Machine learning for neuroimaging with scikit-learn. *Frontiers in Neuroinformatics, 8*, 14. https://doi.org/10.3389/fninf.2014.00014

Appleton, A. A., & Kubzansky, L. D. (2014). Emotion regulation and cardiovascular disease risk. In J. J. Gross (Ed.), *Handbook of emotion regulation* (pp. 596–612). The Guilford Press.

Appleton, A. A., Buka, S. L., Loucks, E. B., Gilman, S. E., & Kubzansky, L. D. (2013). Divergent associations of adaptive and maladaptive emotion regulation strategies with inflammation. *Health Psychology, 32*, 748–756.

Appleton, A. A., Loucks, E. B., Buka, S. L., & Kubzansky, L. D. (2014). Divergent associations of antecedent- and response-focused emotion regulation strategies with midlife cardiovascular disease risk. *Annals of Behavioral Medicine, 48*(2), 246–255. https://doi.org/10.1007/s12160-014-9600-4

Baldassarre, D., Veglia, F., Hamsten, A., Humphries, S. E., Rauramaa, R., de Faire, U., … Group, I. S. (2013). Progression of carotid intima-media thickness as predictor of vascular events: results from the IMPROVE study. *Arteriosclerosis, Thrombosis, and Vascular Biology, 33*(9), 2273–2279. https://doi.org/10.1161/ATVBAHA.113.301844

Barrett, L. F. (2017). The theory of constructed emotion: an active inference account of interoception and categorization. *Social Cognitive*

and Affective Neuroscience, 12(1), 1–23. https://doi.org/10.1093/scan/nsw154

Benjamini, Y., & Hochberg, Y. (1995). Controlling the false discovery rate: a practical and powerful approach to multiple testing. *Journal of the Royal Statistical Society: Series B: Methodological, 57*(1), 289–300.

Berboth, S., Windischberger, C., Kohn, N., & Morawetz, C. (2021). Test-retest reliability of emotion regulation networks using fMRI at ultra-high magnetic field. *Neuroimage, 232*, 117917. https://doi.org/10.1016/j.neuroimage.2021.117917

Buhle, J. T., Silvers, J. A., Wager, T. D., Lopez, R., Onyemekwu, C., Kober, H., Weber, J., & Ochsner, K. N. (2014). Cognitive reappraisal of emotion: A Meta-analysis of human neuroimaging studies. *Cerebral Cortex, 24*, 2981–2990. https://doi.org/10.1093/cercor/bht154

Chambless, L. E., Folsom, A. R., Davis, V., Sharrett, R., Heiss, G., Sorlie, P., Szklo, M., Howard, G., & Evans, G. W. (2002). Risk factors for progression of common carotid atherosclerosis: the Atherosclerosis Risk in Communities Study, 1987-1998. *American Journal of Epidemiology, 155*(1), 38–47. https://doi.org/10.1093/aje/155.1.38

Chida, Y., & Steptoe, A. (2010). Greater cardiovascular responses to laboratory mental stress are associated with poor subsequent cardiovascular risk status: a meta-analysis of prospective evidence. *Hypertension, 55*, 1026–1032. https://doi.org/10.1161/HYPERTENSIONAHA.109.146621

Cohen, B. E., Edmondson, D., & Kronish, I. M. (2015). State of the art review: depression, stress, anxiety, and cardiovascular disease. *American Journal of Hypertension, 28*(11), 1295–1302. https://doi.org/10.1093/ajh/hpv047

DeSteno, D., Gross, J. J., & Kubzansky, L. (2013). Affective science and health: the importance of emotion and emotion regulation. *Health Psychology, 32*, 474–486.

Diedrichsen, J., & Shadmehr, R. (2005). Detecting and adjusting for artifacts in fMRI time series data. *Neuroimage, 27*(3), 624–634. https://doi.org/10.1016/j.neuroimage.2005.04.039

Elliott, M. L., Knodt, A. R., Ireland, D., Morris, M. L., Poulton, R., Ramrakha, S., … Hariri, A. R. (2020). What is the test-retest reliability of common task-functional MRI measures? New empirical evidence and a meta-analysis. *Psycholgoical Science, 31*, 792–806. https://doi.org/10.1101/681700

Elliott, M. L., Knodt, A. R., & Hariri, A. R. (2021). Striving toward translation: strategies for reliable fMRI measurement. *Trends in Cognitive Sciences, 25*(9), 776–787. https://doi.org/10.1016/j.tics.2021.05.008

Ellis, E. M., Prather, A. A., Grenen, E. G., & Ferrer, R. A. (2019). Direct and indirect associations of cognitive reappraisal and suppression with disease biomarkers. *Psychology & Health, 34*(3), 336–354. https://doi.org/10.1080/08870446.2018.1529313

Gianaros, P. J., & Jennings, J. R. (2018). Host in the machine: a neurobiological perspective on psychological stress and cardiovascular disease. *The American Psychologist, 73*(8), 1031–1044. https://doi.org/10.1037/amp0000232

Gianaros, P. J., Marsland, A. L., Kuan, D. C., Schirda, B. L., Jennings, J. R., Sheu, L. K., … Manuck, S. B. (2014). An inflammatory pathway links atherosclerotic cardiovascular disease risk to neural activity evoked by the cognitive regulation of emotion. *Biological Psychiatry, 75*, 738–745. https://doi.org/10.1016/j.biopsych.2013.10.012

Gianaros, P. J., Sheu, L. K., Uyar, F., Koushik, J., Jennings, J. R., Wager, T. D., Singh, A., & Verstynen, T. (2017). A brain phenotype for stressor-evoked cardiovascular reactivity. *Journal of the American Heart Association, 6*, e006053. https://doi.org/10.1161/JAHA.117.006053

Gianaros, P. J., Kraynak, T. E., Kuan, D. C., Gross, J. J., McRae, K., Hariri, A. R., … Verstynen, T. D. (2020). Affective brain patterns as multivariate neural correlates of cardiovascular disease risk. *Social Cognitive and Affective Neuroscience, 15*, 1034–1045. https://doi.org/10.1093/scan/nsaa050

Griffin, S. M., & Howard, S. (2021). Instructed reappraisal and cardiovascular habituation to recurrent stress. *Psychophysiology, 58*(5), e13783. https://doi.org/10.1111/psyp.13783

Gross, J. J. (2014). Emotion regulation: Conceptual and empirical foundations. In J. J. Gross (Ed.), *Handbook of emotion regulation* (pp. 3–20). The Guilford Press.

Gross, J. J., & John, O. P. (2003). Individual differences in two emotion regulation processes: implications for affect, relationships, and well-being. *Journal of Personality and Social Psychology, 85*(2), 348–362.

Grundy, S. M., et al. (2001). Executive summary of the third report of the national cholesterol education program (NCEP) expert panel on detection, evaluation, and treatment of high blood cholesterol in adults (adult treatment panel III). *JAMA, 285*(19), 2486–2497. https://doi.org/10.1001/jama.285.19.2486

Haufe, S., Meinecke, F., Gorgen, K., Dahne, S., Haynes, J. D., Blankertz, B., & Biessmann, F. (2014). On the interpretation of weight vectors of linear models in multivariate neuroimaging. *Neuroimage, 87*, 96–110. https://doi.org/10.1016/j.neuroimage.2013.10.067

Infantolino, Z. P., Luking, K. R., Sauder, C. L., Curtin, J. J., & Hajcak, G. (2018). Robust is not necessarily reliable: from within-subjects fMRI contrasts to between-subjects comparisons. *Neuroimage, 173*, 146–152. https://doi.org/10.1016/j.neuroimage.2018.02.024

Jentsch, V. L., & Wolf, O. T. (2020). The impact of emotion regulation on cardiovascular, neuroendocrine and psychological stress responses. *Biological Psychology, 154*, 107893. https://doi.org/10.1016/j.biopsycho.2020.107893

Jiang, W. (2015). Emotional triggering of cardiac dysfunction: the present and future. *Current Cardiology Reports, 17*(10), 91. https://doi.org/10.1007/s11886-015-0635-3

Kamarck, T., & Jennings, J. R. (1991). Biobehavioral factors in sudden cardiac death. *Psychological Bulletin, 109*(1), 42–75. https://doi.org/10.1037/0033-2909.109.1.42

Koban, L., Gianaros, P. J., Kober, H., & Wager, T. D. (2021). The self in context: brain systems linking mental and physical health. *Nature Reviews. Neuroscience, 22*(5), 309–322. https://doi.org/10.1038/s41583-021-00446-8

Kohoutova, L., Heo, J., Cha, S., Lee, S., Moon, T., Wager, T. D., & Woo, C. W. (2020). Toward a unified framework for interpreting machine-learning models in neuroimaging. *Nature Protocols, 15*(4), 1399–1435. https://doi.org/10.1038/s41596-019-0289-5

Koo, T. K., & Li, M. Y. (2016). A Guideline of Selecting and Reporting Intraclass Correlation Coefficients for Reliability Research. *Journal of Chiropractic Medicine, 15*(2), 155–163. https://doi.org/10.1016/j.jcm.2016.02.012

Kozakova, M., Palombo, C., Morizzo, C., Nolan, J. J., Konrad, T., Dekker, J. M., … Nilsson, P. M. (2013). Gender-specific differences in carotid intima-media thickness and its progression over three years: a multicenter European study. *Nutrition, Metabolism, and Cardiovascular Diseases, 23*(2), 151–158. https://doi.org/10.1016/j.numecd.2011.04.006

Kragel, P. A., Han, X., Kraynak, T. E., Gianaros, P. J., & Wager, T. D. (2021). Functional MRI can be highly reliable, but it depends on what you measure: a commentary on Elliott et al. (2020). *Psychological Science, 32*(4), 622–626. https://doi.org/10.1177/0956797621989730

Kraynak, T. E., Marsland, A. L., & Gianaros, P. J. (2018). Neural mechanisms linking emotion with cardiovascular disease. *Current Cardiology Reports, 20*(12), 128. https://doi.org/10.1007/s11886-018-1071-y

Kubzansky, L. D., Davidson, K. W., & Rozanski, A. (2005). The clinical impact of negative psychological states: expanding the spectrum of risk for coronary artery disease. *Psychosomatic Medicine, 67*(*Suppl 1*), S10–S14.

Kubzansky, L. D., Park, N., Peterson, C., Vokonas, P., & Sparrow, D. (2011). Healthy psychological functioning and incident coronary heart disease: the importance of self-regulation. *Archives of General Psychiatry, 68*(4), 400–408. https://doi.org/10.1001/archgenpsychiatry.2011.23

Lampert, R. (2016). Mental stress and ventricular arrhythmias. *Current Cardiology Reports, 18*(12), 118. https://doi.org/10.1007/s11886-016-0798-6

Lang, P. J., Bradley, M. M., & Cuthbert, B. N. (2008). International affective picture system (IAPS): Affective ratings of pictures and instruction manual. *Technical Report, A-8*.

Lindquist, K. A., Wager, T. D., Kober, H., Bliss-Moreau, E., & Barrett, L. F. (2012). The brain basis of emotion: a meta-analytic review. *Behavioral and Brain Sciences, 35*(3), 121–143. https://doi.org/10.1017/S0140525X11000446

Lorenz, M. W., Markus, H. S., Bots, M. L., Rosvall, M., & Sitzer, M. (2007). Prediction of clinical cardiovascular events with carotid intima-media thickness: a systematic review and meta-analysis. *Circulation, 115*(4), 459–467.

Mackinnon, A. D., Jerrard-Dunne, P., Sitzer, M., Buehler, A., von Kegler, S., & Markus, H. S. (2004). Rates and determinants of site-specific progression of carotid artery intima-media thickness: the carotid atherosclerosis progression study. *Stroke, 35*(9), 2150–2154. https://doi.org/10.1161/01.STR.0000136720.21095.f3

Manuck, S. B., Kaplan, J. R., & Clarkson, T. B. (1983). Behaviorally induced heart rate reactivity and atherosclerosis in cynomolgus monkeys. *Psychosomatic Medicine, 45*, 95–108.

McRae, K., Ciesielski, B., & Gross, J. J. (2012). Unpacking cognitive reappraisal: goals, tactics, and outcomes. *Emotion, 12*(2), 250–255. https://doi.org/10.1037/a0026351

McRae, K., Jacobs, S. E., Ray, R. D., John, O. P., & Gross, J. J. (2012). Individual differences in reappraisal ability: Links to reappraisal frequency, well-being, and cognitive control. *Journal of Research in Personality, 46*(1), 2–7.

Morey, R. D., & Rouder, J. N. (2011). Bayes factor approaches for testing interval null hypotheses. *Psychological Methods, 16*(4), 406–419. https://doi.org/10.1037/a0024377

Ochsner, K. N., Bunge, S. A., Gross, J. J., & Gabrieli, J. D. (2002). Rethinking feelings: an FMRI study of the cognitive regulation of emotion. *Journal of Cognitive Neuroscience, 14*(8), 1215–1229. https://doi.org/10.1162/089892902760807212

Öngür, D., & Price, J. (2000). The organization of networks within the orbital and medial prefrontal cortex of rats, monkeys, and humans. *Cerebral Cortex, 10*, 206–219.

Pedregosa, F., Varoquaux, G., Gramfort, A., Michel, V., Thirion, B., Grisel, O., … Dubourg, V. (2011). Scikit-learn: machine learning in Python. *The Journal of Machine Learning Research, 12*, 2825–2830.

Poldrack, R. A., Huckins, G., & Varoquaux, G. (2020). Establishment of best practices for evidence for prediction: a review. *JAMA Psychiatry, 77*(5), 534–540. https://doi.org/10.1001/jamapsychiatry.2019.3671

Quigley, K. S., Kanoski, S., Grill, W. M., Barrett, L. F., & Tsakiris, M. (2021). Functions of Interoception: from energy regulation to experience of the self. *Trends in Neurosciences, 44*(1), 29–38. https://doi.org/10.1016/j.tins.2020.09.008

Rozanski, A., Blumenthal, J. A., & Kaplan, J. (1999). Impact of psychological factors on the pathogenesis of cardiovascular disease and implications for therapy. *Circulation, 99*(16), 2192–2217.

Steptoe, A., & Brydon, L. (2009). Emotional triggering of cardiac events. *Neuroscience and Biobehavioral Reviews, 33*(2), 63–70. https://doi.org/10.1016/j.neubiorev.2008.04.010

Stewart, J. C., Janicki, D. L., Muldoon, M. F., Sutton-Tyrrell, K., & Kamarck, T. W. (2007). Negative emotions and 3-year progression of subclinical atherosclerosis. *Archives of General Psychiatry, 64*(2), 225–233.

Suls, J. (2018). Toxic affect: are anger, anxiety, and depression independent risk factors for cardiovascular disease? *Emotion Review, 10*, 6–17.

Tattersall, M. C., Gassett, A., Korcarz, C. E., Gepner, A. D., Kaufman, J. D., Liu, K. J., Astor, B. C., Sheppard, L., Kronmal, R. A., & Stein, J. H. (2014). Predictors of carotid thickness and plaque progression during a decade: the Multi-Ethnic Study of Atherosclerosis. *Stroke, 45*(11), 3257–3262. https://doi.org/10.1161/STROKEAHA.114.005669

Tawakol, A., Ishai, A., Takx, R. A., Figueroa, A. L., Ali, A., Kaiser, Y., Truong, Q. A., Solomon, C. J. E., Calcagno, C., Mani, V., Tang, C. Y., Mulder, W. J. M., Murrough, J. W., Hoffmann, U., Nahrendorf, M., Shin, L. M., Fayad, Z. A., & Pitman, R. K. (2017). Relation between resting amygdalar activity and cardiovascular events: a longitudinal and cohort study. *Lancet, 389*, 834–845. https://doi.org/10.1016/S0140-6736(16)31714-7

Tschiderer, L., Klingenschmid, G., Seekircher, L., & Willeit, P. (2020). Carotid intima-media thickness predicts carotid plaque development: meta-analysis of seven studies involving 9341 participants. *European Journal of Clinical Investigation, 50*(4), e13217. https://doi.org/10.1111/eci.13217

Turner, A. I., Smyth, N., Hall, S. J., Torres, S. J., Hussein, M., Jayasinghe, S. U., Ball, K., & Clow, A. J. (2020). Psychological stress reactivity and future health and disease outcomes: A systematic review of prospective evidence. *Psychoneuroendocrinology, 114*, 104599. https://doi.org/10.1016/j.psyneuen.2020.104599

Wagenmakers, E. J. (2007). A practical solution to the pervasive problems of p values. *Psychonomic Bulletin & Review, 14*(5), 779–804. https://doi.org/10.3758/bf03194105

Wager, T. D., Davidson, M. L., Hughes, B. L., Lindquist, M. A., & Ochsner, K. N. (2008). Prefrontal-subcortical pathways mediating successful emotion regulation. *Neuron, 59*(6), 1037–1050. https://doi.org/10.1016/j.neuron.2008.09.006

Willeit, P., Tschiderer, L., Allara, E., Reuber, K., Seekircher, L., Gao, L., … A. S. G. (2020). Carotid intima-media thickness progression as surrogate marker for cardiovascular risk: meta-analysis of 119 clinical trials involving 100 667 patients. *Circulation, 142*(7), 621–642. https://doi.org/10.1161/CIRCULATIONAHA.120.046361

Zaehringer, J., Jennen-Steinmetz, C., Schmahl, C., Ende, G., & Paret, C. (2020). Psychophysiological effects of downregulating negative emotions: insights from a meta-analysis of healthy adults. *Frontiers in Psychology, 11*, 470. https://doi.org/10.3389/fpsyg.2020.00470